EURASIP Journal on Applied Signal Processing 2004:13, 1985–1992

Rapid Binary Gage Function to Extract a Pulsed Signal Buried in Noise

Colin Ratcliffe
Mechanical Engineering Department, United States Naval Academy, Annapolis, MD 21402, USA
Email: ratcliff@usna.edu

William J. Bagaria
Aerospace Engineering Department, United States Naval Academy, Annapolis, MD 21402, USA
Email: bagaria@usna.edu

Sonia M. F. Garcia
Mathematics Department, United States Naval Academy, Annapolis, MD 21402, USA
Email: smg@usna.edu

Richard P. Fahey
Aerospace Engineering Department, United States Naval Academy, Annapolis, MD 21402, USA
Email: rpfahey@usna.edu

Received 1 August 2003; Revised 14 January 2004; Recommended for Publication by Sang Uk Lee

The type of signal studied in this paper is a periodic pulse, with the pulse length short compared to the period, and the signal is buried in noise. If standard techniques such as the fast Fourier transform are used to study the signal, the data record needs to be very long. Additionally, there would be a very large number of calculations. The rapid binary gage function was developed to quickly determine the period of the signal, and the start time of the first pulse in the data. Once these two parameters are determined, the pulsed signal can be recovered using a standard data folding and adding technique.

Keywords and phrases: rapid binary gage function, signal, pulsed signal, noise.

1. INTRODUCTION

The motivation for this research was the need to extract pulsed signals that were buried in noise (signal-to-noise ratio less than one). The signals of interest have a "short" pulse duration compared to the period of the signal, and they are "weak" compared to the background noise. Another consideration when analyzing these signals was that the length of the recorded signal be as short as possible.

Classic techniques for recovering information about noisy signals are usually based on the Fourier transform [1], the periodogram [2], or simply folding and adding the data. When dealing with digitized data, certain precautions must be taken when the data are analyzed. The signal must be digitized based on the Nyquist sampling rate, which in turn is based on the highest desired frequency component of the signal. This is to avoid the appearance of false aliases in the Fourier transform. Generally, to avoid this, the analog signal is first lowpass filtered before being digitized [3].

Difficulties arise when recording and analyzing signals which have a pulse duration that is short when compared to the pulse period. Such a signal contains frequency components that are very high compared to the fundamental frequency of the signal. For pulsed signals, the digitizing rate must be sufficiently high so that the pulse is well defined. This means that the sampling rate is dictated by the pulse duration, and not the period of the signal. The use of filters to precondition this type of signal when it is buried in noise might in fact result in the pulse being completely filtered out of the data. Additionally, when the signal is buried in noise, the classic techniques, when applied to high frequency signals, require long data records. This in turn, necessitates very long times to acquire and analyze the data.

As an example, consider the problem of using signals measured from pulsars as the primary navigation aid for interplanetary travel, which could include the problem of fixing the Earth in its orbit around the sun. One navigational principle is based on using the Doppler shift of the pulsar

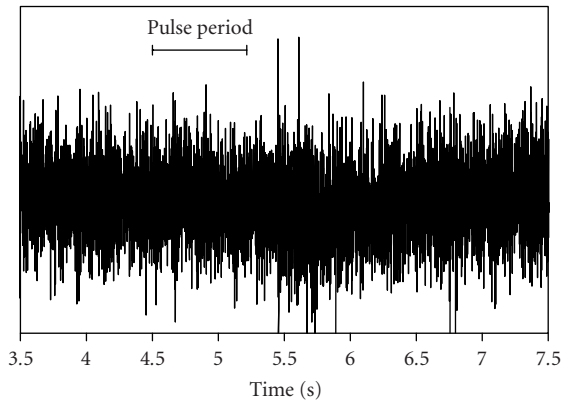

Figure 1: Signal from pulsar PSR B0329 + 54 captured by a 12 m antenna.

pulse rate measured from a number of pulsars. These shifts can be used to identify the direction of travel, and ultimately the position of the Earth or any other interplanetary space vehicle. One candidate pulsar is PSR B0329 + 54, which has a period of 0.715 seconds and a pulse width of approximately 8.7 milliseconds. An example of data captured from this pulsar using a 12-meter parabolic antenna is shown in Figure 1. Data capture for this data set started on 3/3/98 at 21:20:46 GMT, and the sample rate was 1000 samples per second. The time record shown in the figure should include several pulses, but these cannot be seen because the pulsed signal is completely buried in noise.

The spectral resolution of the pulse rate required for satisfactory interplanetary navigation using this pulsar is about 3 μHz. If classical FFT analysis were selected for this problem, the Nyquist sampling rate and FFT theory control the length of an individual time record to 1/(required spectral resolution). For this pulsar the required record length is 330 000 seconds, or nearly 4 days. Clearly, a single data record would be insufficient to extract the pulse from the noise. It is estimated that at least 100 averages would be required for satisfactory extraction. Thus, the total data capture would take at least 33×10^6 seconds, or 385 days. It is impossible to maintain the alignment of a single earthbound dish for this length of time since the rotation of the Earth typically limits data acquisition to less than half a day at a time. This aside, the process would eventually produce an average position of the Earth during data acquisition and the ability to locate the Earth within its orbit is lost. Thus, FFT-based methods cannot be used for this navigational application because the fix time of 385 days is comparable to the journey time!

These and other considerations led to the development of a non-FFT-based technique to recover a pulsed signal buried in noise. The procedure developed in this paper can determine the pulse period using data acquired in only a few minutes, thus permitting close to real-time analysis.

The paper is divided into two parts. First, a method is presented that allows the rapid determination of the period of the signal, and the start time of the first pulse in the data. Second, the time-averaged wave form shape of the pulsed signal is recovered from the noisy data.

2. NOISY DATA

Consider a data signal $D(t)$ which is the sum of a periodic pulsed signal $F(t)$ and noise $N(t)$. Example signals are shown in Figures 2a and 2b.

Notice that the vertical scales of Figures 2a and 2b are different. The pulsed signal, $F(t)$, has a period of T_F. The pulse width, T_F/K_F, is given in terms of the period, and a constant K_F, with K_F being called the pulse width parameter. It is expected that the beginning of the first pulse, in the recorded data, does not start at $t = 0$. The time t_{SF} shifts the pulse in time to account for this. The signal $F(t)$ shown in Figure 2a can be generated using the following equations:

$$F(t) = \begin{cases} A_F \sin\left(\dfrac{\pi K_F}{T_F}\left[(t - t_{SF}) - (C_N - 1)\,T_F\right]\right) & \text{during the pulse,} \\ 0 & \text{outside the pulse,} \end{cases}$$
$$C_N = 1, 2, \ldots, C. \tag{1}$$

In this equation, C_N is the cycle number, C is the maximum number of cycles, and A_F is the maximum amplitude of $F(t)$. The pulse width parameter takes on the values $K_F \geq 1$. If $K_F = 1$, then the pulse width is equal to the period. It is to be noted that K_F probably will not be an integer.

The mean value of a pulsed signal is not necessarily equal to zero. The mean value of the example $F(t)$ is $\bar{f} = 2A_F/\pi K_F$, and is nonzero. Because $\bar{f}$ may not be equal to zero, we do not average out the mean value of $D(t)$ before analyzing the signal as is usually done [4]. This also means that a nonzero mean value of the noise would not be removed.

Mathematically, define

$$F(t) = f(t) + \bar{f},$$
$$N(t) = \nu(t) + \bar{\nu}, \tag{2}$$

where $f(t)$ is the zero-mean time-varying part of the pulsed signal $F(t)$, and $\bar{f}$ is the mean value. The zero-mean time-varying part of the noise, $N(t)$, is $\nu(t)$, and $\bar{\nu}$ is the nonzero mean value. Using the above definitions, the observed data signal is given by

$$D(t) = F(t) + N(t) = f(t) + \bar{f} + \nu(t) + \bar{\nu}. \tag{3}$$

For storage and analysis purposes, the data signal is digitized. The inverse of the sampling rate is h, with units of seconds/sample. The total number of data points is $n = t_R/h$. Here, n is an integer, and t_R is the total time of the record length.

3. DISCRETE CROSS-CORRELATION FUNCTION

The cross-correlation function gives the correlation between two signals, $x(t)$ and $y(t)$. When x and y are digitized, the discrete form of the cross-correlation function is employed. The digitized signals are x_i and y_i with $i = 1, 2, \ldots, n$. The

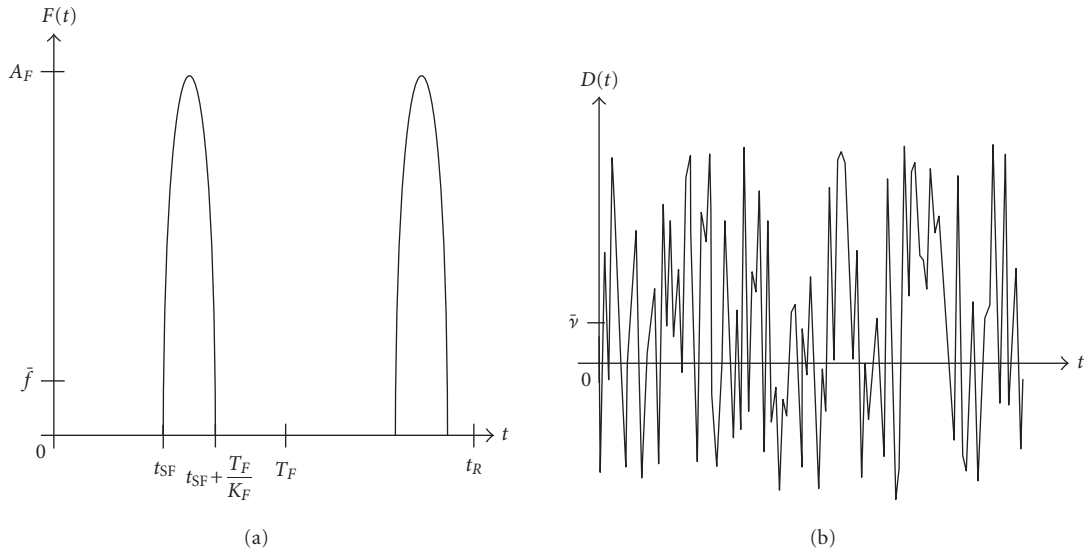

FIGURE 2: (a) Pulsed signal $F(t)$ versus time t. (b) Data signal $D(t) = F(t) + N(t)$ versus time t.

biased discrete cross-correlation function is then given by

$$\hat{R}_{xy}(rh) = \frac{1}{n}\sum_{i=1}^{n-r} x_i y_{i+r}, \quad r = 0, 1, 2, \ldots, m \le n-1. \tag{4}$$

In this equation, r is the lag number. Then rh is the lag time between y and x. The lag time rh is the digital equivalent of the continuous lag time τ. Notice, as r approaches $n-1$ there are fewer and fewer terms which are added together. This results in a loss of accuracy for high lag times [1]. Two important properties of the cross-correlation function, [1, 5], are

$$\begin{aligned} |\hat{R}_{xy}(rh)|^2 &\le \hat{R}_x(0)\hat{R}_y(0), \\ |\hat{R}_{xy}(rh)| &\le \frac{1}{2}[\hat{R}_x(0) + \hat{R}_y(0)]. \end{aligned} \tag{5}$$

In these relationships, $\hat{R}_x$ and $\hat{R}_y$ are the autocorrelation functions of x and y, respectively. Another property arises when both x and y are periodic, with the *same* period. For this special case, the cross-correlation function is also periodic, with the same period as x and y [1]. A significant disadvantage of using the autocorrelation function is the large number of calculations that need to be performed. It requires $(n^2+n)/2$ multiplications, and $(n^2+n)/2$ additions for the direct method, although FFT methods can reduce the number of multiplications to $n \log n$.

4. MODIFIED DISCRETE CROSS-CORRELATION FUNCTION

For the purposes of this research, the discrete cross-correlation function, (4), was modified. The x_i term was replaced with the data, D_i, with $i = 1, 2, \ldots, n$. The y_i term was replaced with a pulsed periodic reference function called the *binary gage*. It is defined as follows:

$$G(t, T, K) = \begin{cases} 0 & \text{outside the pulse,} \\ 1 & \text{during the pulse.} \end{cases} \tag{6}$$

The pulses occur during the times

$$\tau + (C_N - 1)T \le t \le \tau + (C_N - 1)T + \frac{T}{K} \tag{7}$$

with

$$C_N = 1, 2, \ldots, C. \tag{8}$$

Here, T is the period, and K is the pulse width parameter of the binary gage. The binary gage is illustrated in Figure 3. Notice that the binary gage is not a Walsh or related function [1, 6] which are square waves with values of ± 1. The binary gage only takes on the values 0 and 1 and has variable period T and pulse width parameter K.

The binary gage is digitized with the same h value as was used for the data. However, to increase accuracy, it is twice as long as the length of the data set. The digitized binary gage is G_j, with $j = 1, 2, \ldots, n, \ldots, 2n$. Since the binary gage is twice as long as D_i, the summation upper limit in (4) becomes n. Using these substitutions, and multiplying through by n, (4) becomes

$$n\hat{R}_{DG}(rh) = \sum_{i=1}^{n} D_i G_{i+r}, \quad r = 0, 1, \ldots, n-1. \tag{9}$$

The effect of the noise on (9) can be illustrated by substituting $D_i = F_i + \nu_i + \bar{\nu}$. This gives

$$\begin{aligned} &n\hat{R}_{DG}(rh) \\ &= \sum_{i=1}^{n} F_i G_{i+r} + \sum_{i=1}^{n} \nu_i G_{i+r} + \bar{\nu}\sum_{i=1}^{n} G_{i+r}, \quad r = 0, 1, \ldots, n-1. \end{aligned} \tag{10}$$

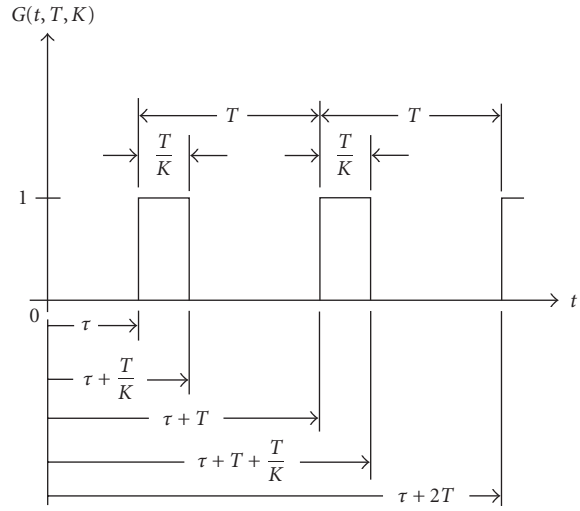

FIGURE 3: The binary gage $G(t, T, K)$ versus time t.

The first term on the right is the cross-correlation of the pulsed signal with the binary gage. When the period of the binary gage is the same as the period of the pulsed signal, the cross-correlation will have the same period. The second term on the right is the cross-correlation of the noise with the binary gage. The pieces of equipment used to receive, digitize, and store the data signal have finite band widths. Thus, ν_i is band-limited white noise (pink noise). This means that the second term on the right will not exactly sum to zero. The third term is a result of the mean value of the noise not being zero. In this equation, it is implied that the noise is stationary and ergodic. Strictly speaking, the noise only has to have these features during the time of the data record.

5. RAPID BINARY GAGE FUNCTION

The purpose of the *rapid binary gage function* (RBGF) is to rapidly determine the period, T_F, of the signal, and the start time, t_{SF}, of the first pulse. The properties of the binary gage are used to reduce the number of computations. During the pulse, the binary gage has a value of one. Thus, there is no need to perform these multiplications. Outside the pulse, the binary gage has a value of zero. Thus, there is no need to perform these multiplications or adds. Equation (9) can now be written as

$$\mathrm{RBGF}(rh, T, K) = \sum_{i(G_{i+r}=1)=1}^{n} D_i, \quad r = 0, 1, \ldots, \frac{T}{h} \le n - 1. \tag{11}$$

The notation "$i(G_{i+r} = 1)$" means to perform the adds only during the pulse of the binary gage. Otherwise, increment i to the next value.

There are significant computational savings for (11) compared to (4) and (9). First, there are no multiplications. Second, the RBGF will be periodic, with the period of $F(t)$, when $G(t)$ has the period of $F(t)$. This means that the maximum lag number r only needs to equal T/h. This results in a further savings of computations. The resulting number of adds is nT/Kh.

The use of the RBGF requires an estimate of K, the pulse width parameter of the binary gage. It also requires estimates of the low, T_L, and high, T_H, values of the period of the binary gage. The behavior of the RBGF is seen when a surface plot is generated. For each K, plot the values of RBGF versus T and rh. When T_L and T_H bracket T_F, there will be a peak in the plot when $T = T_F$ and $rh = t_{SF}$. An algorithm for calculating the RBGF is given in Algorithm 1.

Example RBGF plots are shown in Figures 4, 5, 6, and 7. These plots use the $F(t)$ equation that is shown in Figure 2a. For all of the plots the parameters of $F(t)$ were $A_F = 7$, $T_F = 40$ seconds, $K_F = 4$, $t_R = 393$ seconds; and the parameters of the binary gage were $30 \le T \le 50$ seconds, $0 \le rh \le 30$ seconds. Notice that in all four plots, the vertical axis scale is shortened compared to the other two axes. The purpose of this was to clarify the plots.

For Figure 4, the first pulse of the signal started at $t_{SF} = 0$ seconds, and $K = K_F = 4$. The maximum value of the RBGF is at $T = 40$ seconds, and $rh = 0$ seconds, which correspond to the parameters of $F(t)$. The peak value of the RBGF is over 300, which is about 3 times the values of the lower regions of the plot. Thus, T_K and t_{SF} can easily be found from the location of the peak value of the RBGF using a simple peak finding program.

For Figure 5, the first pulse of the signal started at $t_{SF} = 20$ seconds, and $K = K_F = 4$. The maximum value of the RBGF is at $T = 40$ seconds, and $rh = 20$ seconds, which correspond to the parameters of $F(t)$.

Since the binary gage pulse width parameter, K, is estimated, it may turn out that it is higher or lower than the signal pulse width parameter, K_F. The effects of this are shown in the next two figures.

For Figure 6, $K = 2$ which is one half the value of $K_F = 4$. This means that the binary gage pulse is twice that of the signal pulse. The first pulse of the signal started at $t_{SF} = 20$ seconds. A ridge now appears in the contour plot. The ridge ends at $T = 40$ seconds, and $rh = 20$ seconds, which correspond to the parameters of $F(t)$. Notice that the maximum value is still the same as Figures 4 and 5. This agrees with the theory.

For Figure 7, $K = 8$ which is twice the value of $K_F = 4$, indicating that the binary gage pulse is one half that of the signal pulse. The first pulse of the signal started at $t_{SF} = 20$ seconds. A ridge also appears in this contour plot. The maximum value of the ridge begins at $T = 40$ seconds, and $rh = 20$ seconds, which correspond to the parameters of $F(t)$. Since there are fewer points to add together, the maximum value is lower than in the other three plots. However, the maximum value is still about 3 times larger than the lower values. The ridge can easily be located by using a ridge finding program.

The ridge introduces an ambiguity: which end of the ridge gives the period, T_F, of the signal? The ambiguity can be resolved by doubling the pulse width parameter, K, of the binary gage, and replotting. Figures 4, 5, and 6 show that the RBGF takes on a maximum value for $K \le K_F$.

$D(j)$: read in the magnitudes of the data, put them into the array $D(j)$,
t_R = numeric value of the length of the data record (s),
h = numeric value of the inverse of the signal digitization rate(s/sample),
T_L = numeric value of the lowest period of the binary gage (s),
T_H = numeric value of the highest period of the binary gage (s),
K = numeric value of the binary gage pulse-duration-parameter,
$C = \text{int}(t_R/T_H)$, minimum number of whole cycles in the data record. int$(\cdots)$ = integer,
r max = $\text{int}(T_L/h)$, maximum value of the lag number r,
for $T = T_L$ to T_H step h, set the period of the binary gage,
  for $r = 0$ to r max, set the value of the lag number,
  SUM = 0, SUM = temporary variable for summing,
    for $C_N = 1$ to C, C_N = the cycle number,
    $j_L = \text{int}((r * h + (C_N - 1) * T)/h)$, 1st data point during binary gage pulse,
    $j_H = \text{int}((r * h + (C_N - 1) * T + (T/K))/h)$, last data point during binary gage pulse,
      for $j = j_L$ to j_H, sum the data points during binary gage pulses,
      SUM = $D(j)$ + SUM
      next j
    next C_N
  $rh(r) = r * h$, rh = time lag of binary gage,
  RBGF(rh, T) = SUM, value of the rapid binary gage function,
  next r
next T

Algorithm 1: Rapid binary gage function algorithm.

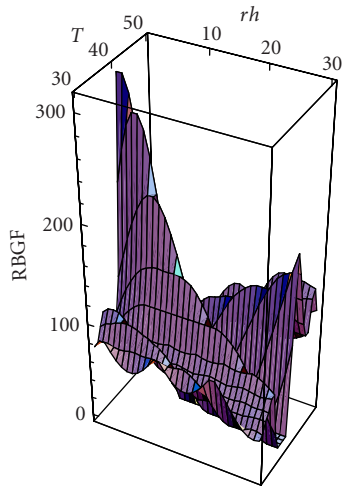

Figure 4: RBGF plot. $T_F = 40$ seconds, $t_{SF} = 0$ second, and $K = K_F = 4$.

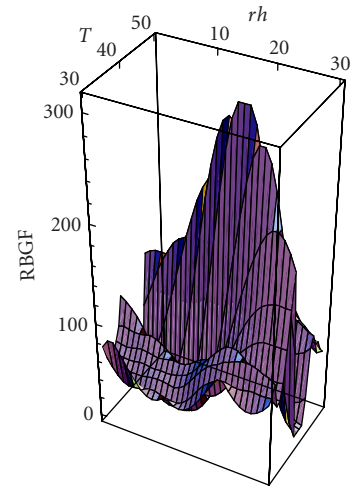

Figure 5: RBGF plot. $T_F = 40$ seconds, $t_{SF} = 20$ seconds, and $K = K_F = 4$.

6. NUMERICAL EXAMPLE

The procedure is demonstrated on a numerically generated signal using parameters comparable to pulsar PSR B0329 + 54. Figure 8 shows part of the 60-second long signal that includes an 8.7-millisecond long half-sine pulse being repeated every 0.7415 seconds, with random noise added. The signal has a pulse width parameter $K_F = 85.2$. Notice that the pulse width is very small compared with the period of the signal. For the reduced data set shown in the figure, there are pulses starting at times of 0.12 seconds and at 0.861 seconds. The data were digitized at a sampling rate of 1000 samples per second. Clearly a simple visual inspection cannot identify the pulses.

The results of applying the RBGF to the full data set are shown in Figure 9. This figure shows data for a broad range of time delays and periods. The original pulse is identifiable as the single large peak.

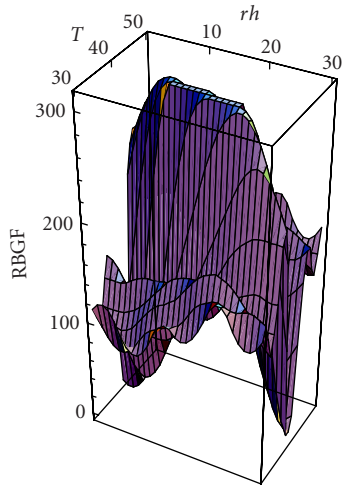

Figure 6: RBGF plot. $T_F = 40$ seconds, $t_{SF} = 20$ seconds, $K = 2$, $K_F = 4$.

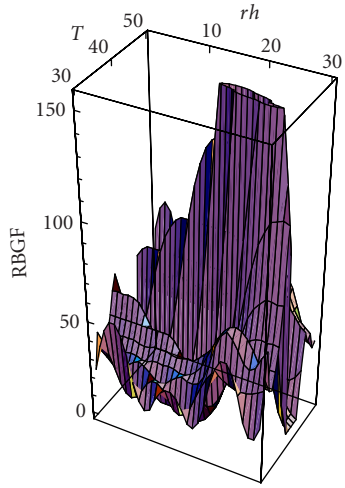

Figure 7: RBGF plot. $T_F = 40$ seconds, $t_{SF} = 20$ seconds, $K = 8$, $K_F = 4$.

For comparison with earlier work in this paper, Figure 10 shows the same results, but with the area of attention focused around the peak of Figure 9. The noise in the signal has caused the peak to lose some of the straightforward form seen in the earlier figures. However, the maximum peak is correctly located at $rh = 0.7415$ seconds and $T = 0.12$ seconds. Thus the RBGF has correctly located the narrow, pulsed signal hidden in significant noise as was shown in Figure 8.

7. RECOVERED AVERAGE WAVE FORM

The signal-to-noise ratio of periodic signals can be increased by summing successive periods of the signal [1]. This is not a correlation process, but an averaging one. In order for the noise to average out, the statistical properties of the noise need to be independent of time during the time of the data record. That is, the noise process must be stationary and ergodic [7].

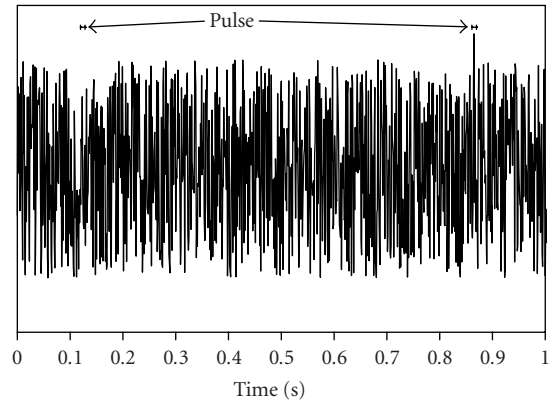

Figure 8: Portion of simulated pulsar data.

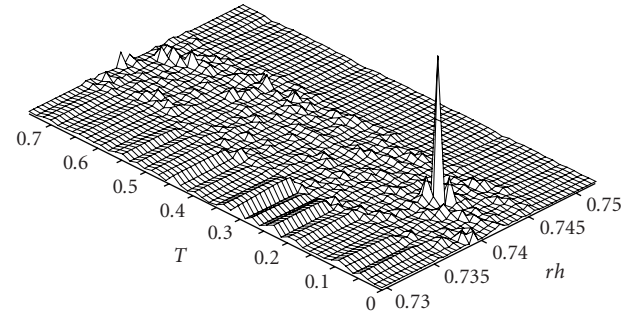

Figure 9: Results of applying the rapid binary gage function to the simulated pulsar data.

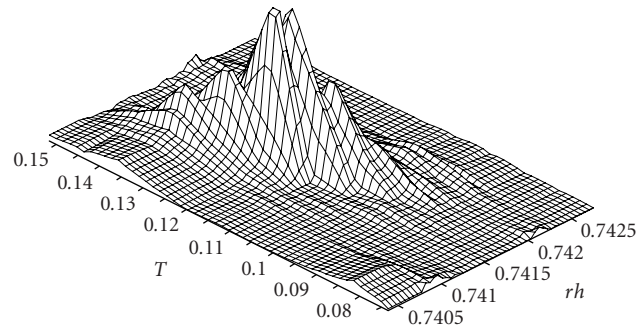

Figure 10: Rapid binary gage function results featuring the region near the peak in Figure 9.

The time averaging process can be illustrated with the help of Figure 11. The wavy line is the amplitude of the recorded data, which includes both the noise and the signal of interest. The RBGF was used to determine the period, T_F, of the periodic signal. Successive cycles in the data are indicated by the vertical dashed lines. The data in each cycle are added to each other, point-by-point. The first data points in each cycle are added to each other. Then the second data points in each cycle are added to each other. This process continues until the last data points in each cycle are added to each other. The results of the averaging process, as applied to the signal shown in Figure 2b, are plotted in Figure 12.

$D(j)$: read in the magnitudes of the data, put it into the array $D(j)$,
h = numeric value of the inverse of the signal digitization rate(s/sample),
T_F = numeric value of the period of $F(t)$ in the data (s) as determined by the RBGF,
t_R = numeric value of the length of the data record (s),
C = int(t_R/T_F), the integer number of whole cycles of $F(t)$ in the data;
for $i = 0$ to int(T_F/h), time of the data point is $t = i * h$ (s),
SUM = 0, temporary variable for summing,
    for $C_N = 1$ to C, C_N = the cycle number,
    sum = $D(i + (C_N - 1) * T_F/h)$ + SUM, sum the data points,
    next C_N
    $Y(i)$ = SUM, magnitude of $Y(t)$,
    $t(i) = i * h$, time,
next i

Algorithm 2: Algorithm to recover $Y(t)$ from the noisy data.

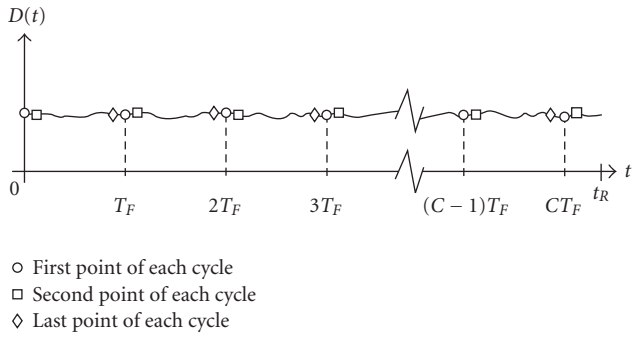

Figure 11: Data $D(t)$ versus time t.

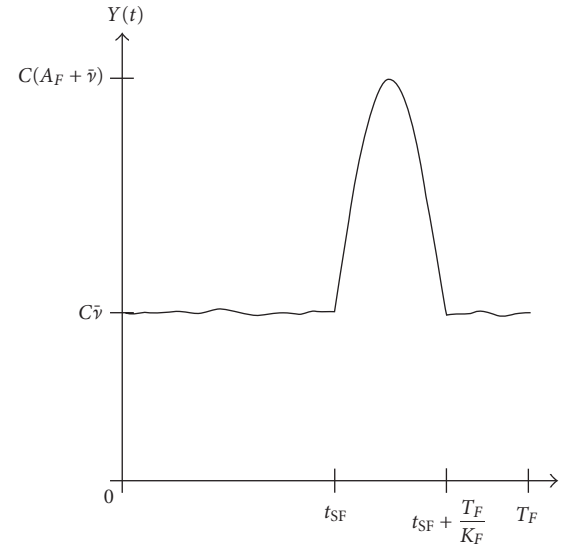

Figure 12: $Y(t)$ versus time t.

The amplitude, $Y(t)$, of the plot is not yet $F(t)$, since C cycles of $F(t)$ were added together, along with C times the mean value of the noise, $\bar{\nu}$. Since the data record is of finite length and the noise is band limited, the noise does not completely average to zero. This results in the slight waviness in the plot. An algorithm to compute $Y(t)$ is given in Algorithm 2. The desired $F(t)$ is derived from $Y(t)$ as follows. The number of whole cycles of $F(t)$ in the data is $C = t_r/T_F$, C being an integer. The magnitude of $C\bar{\nu}$ is determined from the data or the plot. This is subtracted from $Y(t)$ which leaves $CF(t)$. This in turn is divided by C which gives the final signal $F(t)$.

8. CONCLUSIONS

Noisy, pulsed signals of the type studied in this paper require very long data records if conventional techniques are used to analyze them. Additionally, the analysis requires a very large number of calculations. The RBGF was developed to very quickly determine the period of the signal, and the start time of the first pulse in the data, using a relatively short data set. This method works well even when the signal-to-noise ratio is much less than one. Once the period of the signal is determined, a conventional time averaging technique can be used to recover the wave form shape of the signal.

ACKNOWLEDGMENTS

The authors thank Reza Malek-Madani for his insightful help on the use of Mathematica. This research was supported by Naval Research Laboratory Grant N0017398WR00124, Office of Naval Research Grant N0001498WR20010, and the US Naval Academy Research Council.

REFERENCES

[1] K. G. Beauchamp and C. K. Yuen, *Digital Methods for Signal Analysis*, George Allen & Unwin, London, UK, 1979.
[2] T. J. Cavicchi, *Digital Signal Processing*, John Wiley & Sons, New York, NY, USA, 2000.
[3] J. W. Dally, W. F. Riley, and K. G. McConnell, *Instrumentation for Engineering Measurements*, John Wiley & Sons, New York, NY, USA, 2nd edition, 1993.
[4] J. S. Bendat and A. G. Piersol, *Engineering Applications of Correlation and Spectral Analysis*, John Wiley & Sons, New York, NY, USA, 2nd edition, 1993.

[5] R. N. McDonough and A. D. Whalen, *Detection of Signals in Noise*, Academic Press, New York, NY, USA, 2nd edition, 1995.
[6] K. G. Beauchamp, *Applications of Walsh and Related Functions with an Introduction to Sequency Theory*, Academic Press, New York, NY, USA, 1984.
[7] S. L. Marple Jr., *Digital Spectral Analysis with Applications*, Prentice-Hall, Englewood Cliffs, NJ, USA, 1987.

Colin Ratcliffe received his B.A. degree from Sidney Sussex College, Cambridge, UK, in 1977, his M.A. degree from Sidney Sussex College, Cambridge, United Kingdom, in 1981, and his Ph.D. degree from the Institute of Sound and Vibration Research, Southampton University, UK, in 1985. Dr. Ratcliffe's main academic interests lie in the fields of mechanical vibrations and the structural and dynamic analysis of composite structures. He is the inventor of SIDER, *structural irregularity and damage evaluation routine*, which is a vibration-based procedure for rapidly inspecting large composite structures for damage and other features of structural significance. His teaching is predominantly in vibrations, modal analysis, and shock testing, which he teaches both to undergraduate engineering majors and as continuing education courses to industry. He is currently a Professor in the Mechanical Engineering Department at the United States Naval Academy. He is a professional engineer, registered as a Chartered Engineer in London, and is a Member of the Institute of Marine Engineering Science and Technology, London, and the Society for Experimental Mechanics.

William J. Bagaria received his B.S. degree in aeronautical engineering from University of Detroit in 1965, his M.S. degree in mechanical engineering from University of Detroit in 1966, and his Ph.D. degree in engineering mechanics from Michigan State University in 1973. Dr. Bagaria started his professional career, in 1966, working as a structural dynamics engineer on the Saturn V rocket, the Lunar Rover, and the Sky-lab telescope. From 1968 to 1975 he taught at General Motors Institute. From 1975 to 1976 he worked on the General Motors Corporation engineering staff in structural dynamics, and in finite element analysis. In 1976 he began teaching in the Aerospace Engineering Department at the US Naval Academy, where he is currently a Professor Emeritus. Just before he retired from teaching in 2001, he oversaw the structural and mechanical design of the academy's first spacecraft. He is a registered professional engineer in the state of Maryland.

Sonia M. F. Garcia received her B.S. degree in mathematics from Universidade Católica do Paraná, Curitiba, Brazil, in 1974, her M.S. degree in pure mathematics from IMPA, Instituto de Matemática Pura e Aplicada, Rio de Janeiro, Brazil, in 1978, her M.S. degree in mathematics from The University of Chicago, Ill, in 1982, and her Ph.D. degree in mathematics (numerical analysis) from The University of Chicago, Ill, in 1984. Dr. Garcia's main academic interests stretch out in the fields of numerical analysis and applied mathematics. She has been involved with several projects including areas such as solid mechanics, acoustics, and atmospheric physics. For the last three summers Dr. Garcia has been a Visiting Scientist at the Goddard Space Flight Center, NASA. She is currently an Associate Professor of mathematics at the United States Naval Academy. She is currently an eager participant in the new applied mathematics major organization for the Mathematics Department. Her goal is to bring out the importance of the integration of mathematics and all sciences.

Richard P. Fahey received his A.B. degree in philosophy from St. Bonaventure University, St. Bonaventure, NY, in 1964, his M.S. degree in physics (elementary particles) from The Catholic University of America, Washington, DC, in 1968, and his Ph.D. degree in physics (astrophysics) from The Catholic University of America, Washington, DC, in 1980. For the past three decades Dr. Fahey has been developing methods of presenting relativity and quantum theory to nonspecialist audiences. During that time he has taught courses in physics, astronomy, relativity and cosmology, and in the philosophy of nature. His research work includes the spectral analysis of hot, variable stars and galaxies, gravitational wave detection, and the study of relativistic cosmology. Currently he holds the Naval Space Command Research Chair at the US Naval Academy, and is the Deputy Chief of University Programs at NASA's Goddard Space Flight Center.